THE JOURNAL OF BIOLOGICAL CHEMISTRY
Vol. 278, No. 7, Issue of February 14, pp. 5455–5461, 2003

Printed in U.S.A.

Mutational Analyses of the p35-Caspase Interaction

A BOWSTRING KINETIC MODEL OF CASPASE INHIBITION BY p35*

Received for publication, November 14, 2002
Published, JBC Papers in Press, November 27, 2002, DOI 10.1074/jbc.M211607200

Guozhou Xu‡§, Rebecca L. Rich¶, Clemens Steegborn‡, Tongpil Min‡, Yihua Huang‡, David G. Myszka¶, and Hao Wu‡‖

From the ‡Department of Biochemistry, Weill Medical College of Cornell University, New York, New York 10021 and the ¶Center for Biomolecular Interaction Analysis, School of Medicine, University of Utah, Salt Lake City, Utah 84132

Apoptosis is a highly regulated multistep process for programmed cellular destruction. It is centered on the activation of a group of intracellular cysteine proteases known as caspases. The baculoviral p35 protein effectively blocks apoptosis through its broad spectrum caspase inhibition. It harbors a caspase recognition sequence within a highly protruding reactive site loop (RSL), which gets cleaved by a target caspase before the formation of a tight complex. The crystal structure of the post-cleavage complex between p35 and caspase-8 shows that p35 forms a thioester bond with the active site cysteine of the caspase. The covalent bond is prevented from hydrolysis by the N terminus of p35, which repositions into the active site of the caspase to eliminate solvent accessibility of the catalytic residues. Here, we report mutational analyses of the pre-cleavage and post-cleavage p35/caspase interactions using surface plasmon resonance biosensor measurements, pull-down assays and kinetic inhibition experiments. The experiments identify important structural elements for caspase inhibition by p35, including the strict requirement for a Cys at the N terminus of p35 and the rigidity of the RSL. A bowstring kinetic model for p35 function is derived in which the tension generated in the bowstring system during the pre-cleavage interaction is crucial for the fast post-cleavage conformational changes required for inhibition.

The development and homeostasis of multicellular organisms depend on a delicate balance of cell proliferation and programmed cell death or apoptosis. Failure to control either of these processes can lead to serious diseases that threaten the existence of the organism (1, 2). For example, the down-regulation of apoptosis is often associated with cancer, autoimmune disorders, and persistent viral infections. The up-regulation of apoptosis is observed in many forms of degenerative disorders such as Alzheimer's disease, ischemic injury from stroke, and post-menopausal osteoporosis.

The central effectors of apoptotic cell death are caspases, a group of cysteine proteases specific for aspartate residues (3). Caspases are highly regulated at several different levels. First, they are synthesized as inactive single-chain zymogens. Second, caspase activation is achieved through controlled proteolytic cascades, with upstream caspases (Group III, such as caspase-8 and caspase-9) activated by signal-mediated oligomerization and autoprocessing and downstream caspases (Group II, such as caspase-3 and casapse-7) activated by upstream caspases. While caspases have a dominant requirement for Asp at the P1 position, neighboring sequences at P5-P1′ (in particular P4-P2) influence the substrate specificity of each group of caspases (4).

Active caspases are in addition subject to inhibition by specific viral and cellular caspase inhibitors (5, 6). Most notably, the p35 protein from baculoviruses is an effective and the only wide-spectrum caspase inhibitor. It blocks apoptosis induced by numerous stimuli and in diverse organisms (7–9). Transgenic expression of p35 shows immense promise in controlling apoptosis and degenerative diseases (10–20). Previous biochemical and structural studies showed that caspase inhibition by p35 requires the cleavage of a caspase recognition sequence ($DQMD^{87}$) within a solvent exposed and highly protruding reactive site loop (RSL)[1] (21), followed by the formation of a tight post-cleavage complex with the caspase.

Previously, we reported the crystal structure of the post-cleavage complex between p35 and caspase-8, a group III initiator caspase involved in Fas-mediated apoptosis (22). The structure revealed that the caspase is inhibited via a covalent thioester linkage between the active site Cys^{360} of caspase-8 (Cys^{285} of caspase-1 numbering) and the cleavage residue Asp^{87} of p35. During normal substrate cleavage, the thioester intermediate is quickly hydrolyzed by an enzyme bound water molecule. In the p35-caspase-8 complex, the thioester bond is preserved by the N terminus of p35, which interacts with the caspase active site and excludes solvent from the catalytic His^{317} of caspase-8 (His^{237} of caspase-1 numbering). The interaction between the p35 N terminus and the caspase is realized through a series of dramatic post-cleavage conformational changes (22).

In the structure of the p35-caspase-8 post-cleavage complex, three regions of p35 directly contact the caspase, the N terminus, the KL region (including the KL loop and the K and L strands) and the substrate sequence of p35 (Fig. 1). To further understand the structural determinant of caspase inhibition by p35, we performed structure-based mutagenesis at these three regions of p35. The mutants were extensively analyzed for their effects on the pre-cleavage association, as assessed by surface

* This work was supported in part by National Institutes of Health Grant AI50872 (to H. W.). The costs of publication of this article were defrayed in part by the payment of page charges. This article must therefore be hereby marked "*advertisement*" in accordance with 18 U.S.C. Section 1734 solely to indicate this fact.

§ Present address: Immunology Program, Sloan-Kettering Division, Weill Graduate School of Medical Sciences of Cornell University, New York, NY 10021.

‖ Pew scholar of biomedical sciences and a Rita Allen Scholar. To whom correspondence should be addressed: Dept. of Biochemistry, Weill Medical College of Cornell University, Whitney-2, 1300 York Ave., New York, NY 10021. Tel.: 212-746-6451; Fax: 212-746-4843; E-mail: haowu@med.cornell.edu.

[1] The abbreviations used are: RSL, reactive site loop; Ac-DEVD-AFC, acetyl-Asp-Glu-Val-Asp-7-amino-4-trifluoromethylcoumarin; CHAPS, 3-[(3-cholamidopropyl)dimethylammonio]-1-propanesulfonic acid.

plasmon resonance biosensor measurements, and on the post-cleavage inhibition, as determined by both qualitative pull-down assays and quantitative kinetic inhibition experiments. These experiments not only identified functionally important structural elements of p35 in caspase inhibition, but also led to a novel bowstring kinetic model of caspase inhibition by p35. In this model, the p35 may be considered as a bowstring system with the RSL being the string. The tension produced in the string during the pre-cleavage association with a target caspase appears to control the efficiency of caspase inhibition by facilitating fast post-cleavage conformational changes.

EXPERIMENTAL PROCEDURES

Protein Expression and Purification—Wild-type and mutant baculoviral p35 (residues 1–299, with a C-terminal His-tag), human caspase-8 (residues Ser^{201}–Asp^{463}, with or without a C-terminal His-tag), human caspase-3 (residues 1–277, with or without a C-terminal His-tag), and human caspase-3 active site mutant (C163A, with a C-terminal His-tag) were expressed in the pET bacterial expression system using overnight isopropyl-1-thio-β-D-galactopyranoside induction at 20 °C. The His-tagged proteins were purified by nickel (nickel-nitrilotriacetic acid) affinity and gel-filtration chromatography. Both caspase-8 and caspase-3 were autoprocessed to their mature forms during the protein expression and purification procedures. To generate the mature form of the mutant caspase-3 (C163A), the cell pellets of His-tagged caspase-3 (C163A) were mixed with those of non-tagged caspase-8. The mixed cells were lysed by sonication and incubated for 30 min at room temperature to allow the processing of caspase-3 (C163A) by the active caspase-8 in the lysate.

His-tag Pull-down Assay—Purified His-tagged wild-type or mutant p35 proteins were mixed with cell pellets of non-tagged caspase-8 or caspase-3 and lysed in 20 mM Tris at pH 7.4, 150 mM NaCl, 10 mM imidazole, and 10 mM β-mercaptoethanol. Pre-equilibrated nickel-nitrilotriacetic acid resins were incubated with the mixtures at 4 °C overnight and washed three times with the same buffer. The bound proteins were eluted using 250 mM imidazole and analyzed on SDS-PAGE.

Kinetic Analysis—Caspase inhibition by p35 was assayed by progress curve analysis as described earlier (9). The fluorogenic caspase substrate Ac-DEVD-AFC was purchased from Enzyme Systems. Fluorescence detection upon substrate cleavage by caspases was carried out on a SpectraMax Gemini plate reader using an excitation wavelength of 400 nm and an emission wavelength of 505 nm. The Ac-DEVD-AFC substrate (200 μM) and various concentrations of p35 mutants were first added to the 100-μl reaction wells in a buffer containing 50 mM Hepes at pH 7.4, 100 mM NaCl, 10 mM dithiothreitol, 0.1% (w/v) CHAPS, and 10% sucrose and equilibrated at 37 °C for 20 min. The reactions were initiated by adding pre-warmed caspase-8 or caspase-3 to the mixtures and the substrate hydrolyzes, expressed as relative fluorescence units, were monitored at 20-s intervals for 60–90 min. The final concentrations of caspase-8 and caspase-3 were 0.1 and 1 nM, respectively. The concentration series of p35 used for caspase-8 were 0.01, 0.05, 0.07, 0.1, and 0.3 μM, while those for caspase-3 were 0.01, 0.03, 0.05, 0.07, and 0.1 μM. If no inhibition was observed under these conditions, the analyses were repeated with p35 concentration series of 0.1, 0.3, 0.5, 0.7, and 1.0 μM for either caspase-3 or caspase-8.

As the p35 concentrations were kept at a large excess over caspases, the reactions were rendered pseudo-first order for convenience of analysis (9). The apparent inhibitory constant in the presence of substrate, $K_{i(app)}$, is given by the linear regression as shown in the following equation,

$$\nu_0/\nu_i = 1 + [I]/K_{i(app)} \quad \text{(Eq. 1)}$$

where ν_0 and ν_i are the steady state rates of substrate hydrolysis in the absence and presence of p35 concentration [I], respectively. The K_i can be converted from $K_{i(app)}$ by the following equation,

$$K_i = K_{i(app)}/(1 + [S]/K_m) \quad \text{(Eq. 2)}$$

where [S] is the substrate concentration, and K_m is the kinetic parameter of caspase-3 or caspase-8 for the Ac-DEVD-AFC substrate (9).

Biosensor Measurement—All surface plasmon resonance biosensor measurements were performed using a BIACORE 2000 equipped with a research-grade B1 sensor chip. Mature active-site mutant of caspase-3 (C163A) was immobilized on one flow cell of the sensor chip using amine-coupling chemistry to a surface density of ~200 resonance units. Another activated flow cell was blocked with a 7-min injection of 1 M ethanolamine, pH 8.0. To collect kinetic binding data, concentration series of each p35 protein, in 10 mM Hepes, 300 mM NaCl, 3 mM EDTA, 5 mM dithiothreitol, and 0.05% P20 at pH 7.4, were injected for 30 s over the flow cells at 25 °C using a flow rate of 50 μl/min. No regeneration of the ligand surface was required between injections.

All response data were double-referenced (23), thereby correcting for bulk refractive index changes and nonspecific p35 binding to the sample and reference surfaces. Data were fit globally to a simple interaction model (A + B = AB) using CLAMP (24). For weak interactions, response data sets were fit simultaneously with the wild-type p35 data to obtain more accurate affinity constants.

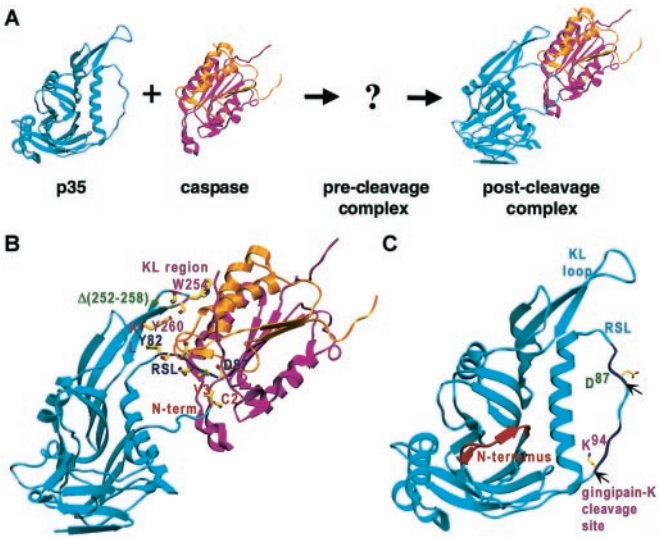

FIG. 1. **p35 structures.** *A*, the potential pathway of caspase inhibition by p35 through the formation of pre-cleavage and post-cleavage complexes. Only half of the complex (a full complex contains a heterotetrameric caspase with two p35 molecules) is shown. *B*, the three regions of p35 in contact with caspase-8 in the p35-caspase-8 post-cleavage structure. *Magenta* and *orange*, large and small subunits of caspase-8; *cyan*, p35. Segments of p35 in contact with caspase-8 are shown in *red* for the N-terminal residues, *blue* for the RSL residues, *magenta* for the KL region residues, and *green* for location of the deletion mutant. *C*, free p35 structure showing the buried N terminus and the cleavage sites for caspases and for the caspase-like protease gingipain-K.

RESULTS AND DISCUSSION

Caspase inhibition by p35 presumably proceeds through two distinct steps: a pre-cleavage association, which is the reversible mutual recognition between p35 and the caspase, followed by the cleavage, and the formation of an irreversible post-cleavage complex (Fig. 1*A*). To obtain a thorough understanding on the mechanism of caspase inhibition by p35, we mutated a series of p35 residues in contact with caspase-8 in the post-cleavage complex, including the p35 N terminus, the KL region and the RSL (Fig. 1*B*). These mutants were characterized to derive an integral understanding of the inhibitory process.

Kinetic Characterization of the Pre-cleavage Association—To trap the pre-cleavage interaction, we used an active site mutant of caspase-3 (C163A) that was processed to its active conformation through trans-activation by its upstream caspase, caspase-8. Measurement by surface plasmon resonance for the interaction between p35 and caspase-3 (C163A) gave rise to an association rate of $6.7 \times 10^5\ M^{-1}\ s^{-1}$, similar to many diffusion-controlled rigid body macromolecular associations (25, 26), and a dissociation rate of $0.091 s^{-1}$ (Table I). This fast rate of association suggests that the interaction between p35 and a caspase does not involve complex conformational changes, which would otherwise slow down the interaction. The calculated equilibrium dissociation constant is 0.13 μM, which is ~200-fold stronger than the K_m between caspase-3 and a peptide substrate (9). Because the direct contact between p35

TABLE I
Biochemical characterization of structure-based p35 mutants

			Cleavage		Post-cleavage interaction				Pre-cleavage interaction		
					Pull-down		K_i				
		Aggregation[a]	Caspase-8	Caspase-3	Caspase-8	Caspase-3	Caspase-8	Caspase-3	k_{on}, caspase-3	k_{off}, caspase-3	K_d, caspase-3
p35	WT	−	+	+	+	+	0.15 nM, relative 1.0	0.87 nM relative 1.0	$6.7 \pm 0.6 \times 10^5$ $M^{-1}s^{-1}$, relative 1.0	0.091 ± 0.012 s^{-1}, relative 1.0	0.13 ± 0.1 μM, relative 1.0
N-terminal region	C2S	−	+	+	−	−			1.0	1.3	0.91
	C2A	−	+	+	−	−			1.3	1.1	0.83
	C2G[b]	−	+	+	−	−			1.2	1.3	1.2
	Δ2–5[b]	+	+	+	−	−			NF[c]	NF	NF
	V3G[b]	+	+	+	−	−			NF	NF	NF
	V3A	+	+	+	−	−			NF	NF	NF
	V3I	−	+	+	+	+	2.1	1.1	1.1	1.0	0.94
	I4A	+	+	+	−	−			NF	NF	NF
	F5A	+	+	+	−	−					
	P6A	+	+	+	−	−					
	D10A	−	+	+	+	+	4.1	2.3	1.1	1.2	1.0
	Q13G	−	+	+	+	+	4.7	1.4	1.1	1.3	1.2
	ΔD10	+	+	+	−	−					
	Δ (10–11)	+	+	+	−	−					
	D10∇G	−	+	+	+	+	15	14	0.83	0.91	1.1
	D10∇GG	+	+	+	−	−			NF	NF	NF
KL-loop region	S253A	−	+	+	+	+	3.9	1.8	0.94	1.0	1.1
	W254A	−	+	+	+	+	12	2.5	0.57	2.0	3.4
	K256A	−	+	+	+	+	3.4	1.3	0.81	2.0	3.4
	Y260A	−	+	+	+	+	19	4.1	0.76	1.4	1.8
	Δ252–258	−	+	+	−	−			0.87	4.1	4.6
	Δ253–257	−	+	+	+	+	13	1.5	1.1	0.82	0.73
	ΔW254	−	+	+	+	+	13	1.6	1.1	1.2	1.1
	253/254/260/AAA	−	+	+	+	+	36	2.1	1.2	1.3	1.1
Substrate region	Y82A[a]	−	+	+	−	−					
	S83A	−	+	+	+	+	1.9	2.8	1.3	2.6	1.9
	D84A	−	+	+	+	+	58	93	0.051	8.3	158
	D84N	−	+	+	+	+	47	61	0.14	13	92
	Q85A	−	+	+	+	+	55	2.8	0.97	3.2	3.3
	Q85K	−	+	+	+	+	400	5.9	0.76	6.3	8.1
	Q85E	−	+	+	+	+	3	1.5	0.85	0.92	1.1
	Q85N	−	+	+	+	+	149	1.3	0.88	8.3	9.2
	M86A	−	+	+	+	+	37	3.1	0.97	1.6	1.7
	M86Q	−	+	+	+	+	21	7.2	0.73	7.2	10
	M86V	−	+	+	+	+	7.3	1.1	0.49	0.047	0.092
	M86I	−	+	+	+	+	13	4.9	0.51	0.23	0.43
	88–91/AAAA	−	+	+	+	+					

[a] Shown by gel filtration.
[b] Previously published mutants (22).
[c] NF, the Biosensor data could not be fit with single bimolecular interaction.

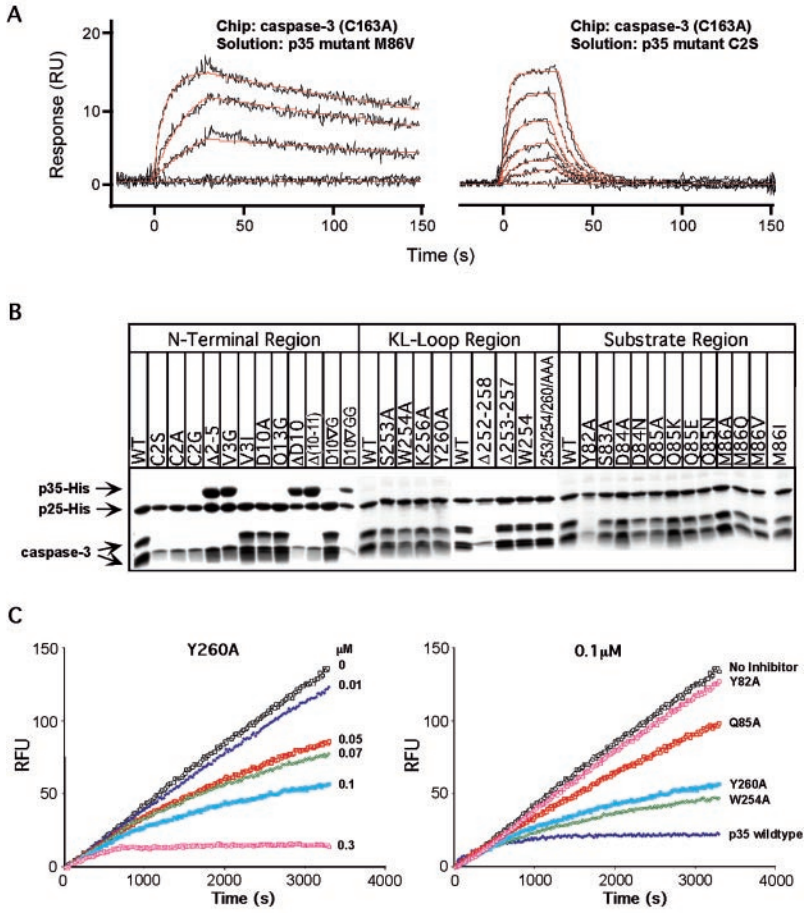

FIG. 2. **Biochemical characterization of caspase inhibition by p35.** *A*, selected examples of the kinetic analysis of the pre-cleavage interaction between p35 and active site mutant of caspase-3 (C163A) using Biacore. *Black lines* represent the responses obtained for 0, 0.033, 0.1, and 0.3 μM p35 mutant M86V (*left*) and 0, 0.016, 0.031, 0.063, 0.13, 0.25, and 0.50 μM p35 mutant C2S (*right*), flowed across caspase-3 (C163A) immobilized on the biosensor surface. *Red lines* indicate the fit of the data to a simple bimolecular interaction model. *B*, pull-down of caspase-3 by wild-type and mutant His-tagged p35. The large subunit of caspase-3 often ran as a close doublet and the p10 fragment of cleaved p35 ran closely to the small subunit of caspase-3. *C*, selected examples of progress curve analyses showing substrate hydrolysis (represented by relative fluorescence units (*RFU*)) with time for caspase-8 inhibition by different concentrations of the p35 mutant Y260A (*left*) and for an overlay of caspase-8 inhibition by wild-type and several p35 mutants at 0.1 μM concentration (*right*).

and a caspase during pre-cleavage interaction is likely not much more extensive than substrate recognition by a caspase (since the KL loop does not appear to be energetically indispensable, see below), the stronger interaction between p35 and a caspase is likely due to the decrease in entropic loss often associated with the recognition of flexible peptide substrates. These kinetic and thermodynamic observations are consistent with the apparent rigidity of the highly solvent accessible RSL in the free p35 structure (21) (Fig. 1*C*).

Strict Requirement of the Cys^2 Residue and Importance of the Structural Integrity of the N-terminal Segment in Free p35—In the crystal structure of the p35/caspase-8 complex, the N terminus of p35 repositions into the active site of caspase-8 to block thioester bond hydrolysis (22). Two p35 N-terminal residues, Cys^2 and Val^3, directly contact the caspase and both the C2G and V3G mutations have been shown to render p35 defective in caspase inhibition (22). To further understand the structural requirement of these two contacting residues, we performed both alanine mutations and conservative substitutions on these residues (Table I, Fig. 2, *A* and *B*).

Similar to the phenotype of the C2G mutation, both C2A and the isosteric C2S mutants failed to pull-down with either caspase-3 or caspase-8, although both were cleaved efficiently by the caspases. As these mutants exhibited identical solution behavior with wild-type p35, as shown by gel-filtration profiles, the mutational effects are likely due to the direct deletion of interactions with the caspases. The drastic phenotype of the C2S mutant suggests that the interaction between residue Cys^2 of p35 and a target caspase exhibits a strict specificity. This specificity may be explained by the structural observation that the side chain thiol of Cys^2 may form a hydrogen bond with the imidazole ring of His^{317} in caspase-8 (22). None of these mutations affected the pre-cleavage association.

Conservative substitution V3I did not significantly change its inhibitory activity against caspases. In contrast, the V3A mutant failed to form a stable complex with either caspase-3 or caspase-8, although it could be readily cleaved by these caspases. Since Val^3 is buried in the free p35 structure, this mutant phenotype may be explained by either a direct effect on a p35-caspase complex or an indirect effect through perturbation of the free p35 structure. Although it is not possible to distinguish these effects, the fact that the V3A mutant tends to aggregate in solution supports that structural perturbation may be at play in this mutant.

To determine whether residues at the N-terminal segment that do not directly contact the caspase (residues 4–13) can influence the ability of p35 to inhibit caspases through structural perturbation, we selectively mutated a few residues at the N terminus. Most N-terminal residues such as Ile^4, Phe^5, and Pro^6 are buried in the free p35 structure, with the exception of Asp^{10} and Gln^{13}. Interestingly, the I4A, F5A, and P6A mutations in p35 were detrimental to the inhibition, while the D10A

and Q13G mutants behaved similarly as the wild-type p35 in their ability to inhibit either caspase-3 or caspase-8. The I4A, F5A, and P6A mutants showed aggregation in their gel-filtration profiles and therefore may have possible local structural perturbations. Accordingly, biosensor measurements showed that the pre-cleavage association of these p35 mutants to caspase-3 (C163A) exhibited complex behavior, indicating the presence of a mixture of stoichiometries in the interactions. In contrast, both the D10A and Q13A mutants behaved as the wild-type p35 in solution. These results support that structural perturbation of the buried N-terminal arm in the free p35 structure can abrogate the inhibitory activity of p35.

The KL Region Makes Modest and Variable Energetic Contribution to Caspase Interaction but Supports a Crucial Contact with the RSL—In the structure of the p35-caspase-8 complex, residues in the KL region make direct contact with residues 414–427 in the small subunit of caspase-8 at the L4 loop and the α4 helix. However, these residues in caspase-8 only show limited sequence conservation among different caspases. Since there are significant conformational changes in the KL loop region between the bound and the free p35, we had earlier proposed that this flexibility of the KL loop might be important for its ability to interact with different caspases (22).

We created a series of point mutations and deletions to determine the functional role of the KL region (Table I and Fig. 2, *B* and *C*). We generated single-site mutations on residues in direct contact with caspase-8, S253A, W254A, K256A, and Y260A. We also created triple alanine mutations on S253, W254, and Y260, the three residues that show most extensive surface area burial in the complex. In addition, we created deletion mutations that remove one (ΔTrp^{254}), five ($\Delta 253–257$) and seven ($\Delta 252–258$) residues from the KL loop and the adjoining β strands.

Surprisingly, the mutational data suggest that the KL loop does not seem to play an indispensable role as would have been predicted from the structure. The W254A, Y260A, ΔTrp^{254}, and $\Delta 253–257$ mutants exhibited only modest, but significant, effects against caspase-8 and behaved essentially as wild-type against caspase-3, an effector caspase. In addition, the pre-cleavage interactions between the p35 mutants and caspase-3 (C163A) are also very similar to the wild-type interaction. These results show that the KL region is not crucial for caspase inhibition and suggest that there may be significant differences in the role of the KL region against different caspases. Interestingly, a low resolution structure of the complex between p35 and an insect effector caspase showed that there is an orientational difference between the p35 in complex with an initiator caspase, caspase-8, and with the effector caspase (27). Although the KL region appears to contact the target caspase in both complexes, their energetic roles may be different.

The relative unimportance of the KL region also explains the ability of p35 to inhibit gingipain-K, a caspase-like bacterial cysteine protease that cleaves a different site on the RSL of p35 (28) (Fig. 1*C*). Because gingipain-K cleaves further downstream (^{91}DSIK^{94}) from the caspase recognition site (^{84}DQMD^{87}), it is unlikely that gingipain-K would be close enough to the KL loop for a direct interaction.

Interestingly, the KL loop deletion mutant $\Delta 252–258$ completely abolished the inhibitory activity of p35 against both caspase-3 and caspase-8, without drastically affecting the formation of the pre-cleavage complex. We have previously shown that residue Tyr^{82} near the beginning of the RSL is essential for the ability of p35 to inhibit caspases (22). We had postulated that Tyr^{82} helps to glue the RSL with the neighboring KL strands, in addition to its role in direct caspase contact. Because mutant $\Delta 253–257$ does not exhibit a drastic decrease in caspase inhibition, and the two additional residues deleted in $\Delta 252–258$ do not directly contact the caspase, the defective phenotype of the $\Delta 252–258$ mutant may be best explained by the perturbation of the local conformation of the K and L strands. Among other interactions, the K and L strands harbor two large aromatic residues Phe^{248} and Trp^{262} that interact with Tyr^{82} of the RSL. As the Cα distance between residues 251 and 259 is 5.2 Å, longer than a typical Cα distance between two adjacent residues, the deletion mutant $\Delta 252–258$ has to undergo conformational changes to join these two residues, leading to structural perturbations. Therefore, a crucial role of the KL region appears to provide a proper "glue" patch for the RSL.

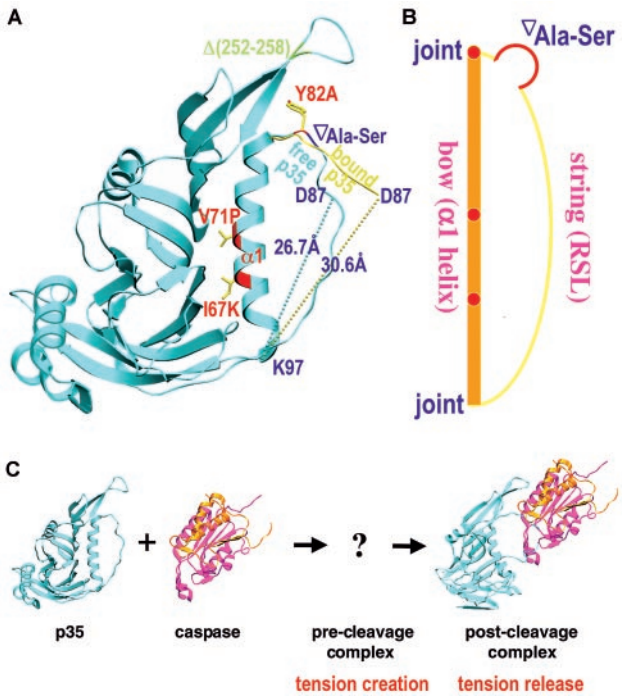

FIG. 3. **Bowstring kinetic model of caspase inhibition by p35.** *A*, mapping of known "tension" mutations on free p35 (*cyan*). The conformation of the bound/cleaved p35 RSL is superimposed (*yellow*). Y82A and $\Delta 252–258$ may compromise the interaction between the RSL and strands K and L at the joint of the bowstring (see *B*); I67K and V71P may weaken the helix or disrupt the interaction of the α1 helix with the β sheet core; the Ala-Ser insertion in the RSL may loose the tension. The potential "stretching" of the RSL is shown by the increased distance between the cleavage residue Asp^{87} and Lys^{97} at the base of the RSL upon caspase interaction. *B*, the bowstring model. *C*, the pathway of caspase inhibition by p35 showing the hypothesis that tension is generated upon pre-cleavage interaction and released upon cleavage.

Substrate Region Residues; Pre-cleavage Association Directly Affects Inhibition, but May Not Be Rate-limiting—The non-covalent interaction between p35 and caspase-8 centers around the tetrapeptide caspase recognition sequence (P4-D^{84}QMD^{87}-P1) in the reactive site loop of p35. It has been shown previously that the P1 Asp residue is essential for p35 function (21, 29), consistent with the absolute specificity of caspases to cleave after Asp residues. To elucidate the specific role of these residues in the function of p35, we generated a series of point mutations at the P2-P4 positions of the caspase recognition sequence.

None of the mutations on the P2-P4 positions completely abolished the caspase inhibitory activity of p35, but produced a range of different effects against caspase-3 and caspase-8 (Table I and Fig. 2) that are largely consistent with the substrate specificity of these caspases (30). For example, mutations on the P2 residue are relatively mild against both caspases, consistent with P2 being the most tolerable. In contrast, P4 mu-

tations are more drastic, especially for caspase-3, which is consistent with the known preference of Asp in this position for the group II apoptotic effector caspases such as caspase-3. The most surprising is the mutational phenotype on the P3 residue, which generated drastic effects on caspase-8, but did not seem to harm its inhibition on caspase-3, even though both caspases appear to prefer Glu at this position based on combinatorial substrate analyses (3, 30).

How does the strength of pre-cleavage association affect the post-cleavage caspase inhibition? It appears that an efficient pre-cleavage interaction is required for inhibition because most of the p35 mutants that have a decreased pre-cleavage interaction are also less effective in caspase inhibition. However, substrate recognition or pre-cleavage interaction seems not to be the rate-limiting step in caspase inhibition by wild-type p35, as exemplified by the M86V mutant, which exhibits significantly stronger pre-cleavage association, but is wild-type in inhibition.

Bowstring Kinetic Model of p35 Inhibition—The molecular event following p35 cleavage suggests the existence of two opposing forces in caspase inhibition by p35. As the post-cleavage strand of p35 departs the active site of the caspase, a series of cooperative conformational changes occur in p35 that allows the release of its N terminus from the core of p35 for interacting with the caspase active site. This has to occur before the caspase is able to hydrolyze the thioester intermediate formed between the caspase and p35. The existence of such a race between the catalytic power of the caspase and the rate of post-cleavage conformational changes may be exemplified by the observed leakage in caspase inhibition by p35, which often requires higher than stoichiometric quantity of p35 to completely inhibit a target caspase (9). In addition, since stronger pre-cleavage association does not necessarily translate into stronger inhibition, the rate-limiting step of the inhibition could rest on the rate of these post-cleavage conformational changes.

So what controls the rate of conformational changes and therefore the efficiency of caspase inhibition? A most conspicuous feature of the free p35 structure is the conformational rigidity of the entirely solvent exposed RSL, as shown by the visibility of the loop in the electron density map (21). In addition, our measurements on the association rate and the strength of the pre-cleavage association also suggest a nearly rigid-body interaction between p35 and the caspase.

During the pre-cleavage association in which the caspase recognition sequence in RSL interacts with the active site of the caspase, this rigidity is likely to transform into tension in the RSL, because RSL residues after the cleavage site would have to be stretched by 4 Å due to the pinching of the caspase recognition sequence (Fig. 3*A*). The Cα distance between the cleavage residue Asp^{87} and Lys^{97} is 26.7 Å in the free p35 structure. Assuming that residue Lys^{97} does not move significantly in the pre-cleavage complex, this distance may be increased to 30.6 Å, which would very likely create tension in this already rigid RSL.

The rigidity and tension in the RSL suggest that p35 might function analogously as a bowstring system for shooting arrows (Fig. 3*B*). In this model, the RSL may be considered as a string and the remainder of p35, especially the long base helix α1, the bow. During the pre-cleavage association, the string is pulled by the caspase and the tension generated may distribute to the entire bowstring system, possibly causing a bent in the base helix. Upon cleavage of the RSL, similarly as in shooting arrows upon release of the string, this stored energy in the bowstring system will pull the part of the RSL after the cleavage site toward the bow and facilitate fast conformational changes.

Based on this bowstring model, for p35 to function efficiently, mutations that compromise the integrity of the bowstring system of p35 will be detrimental. Consistent with this prediction, mutations that weaken the association between the RSL and the p35 bow (Y82A and Δ252–258), mutations that weaken the integrity of the base helix (V71P and I67K) (21, 31), and an insertion mutation that lengthens the string (insertion of Ala-Ser after residue 83) (29), all abolish caspase inhibition by p35. This tension model is further supported by the structural similarity between the cleaved structure of an inhibition-defective p35 mutant V71P and the cleaved structure of wild-type p35 as in complex with caspase-8 (22, 32). This similarity suggests that the V71P mutant does not have a gross structural defect but exhibits a tension defect due to a weaker base helix.

Mechanistic Similarities to Serpins—Besides p35, the only other known case of covalent inhibition or suicide inhibition by protease inhibitors is mediated by serpins, a family of inhibitors mostly for serine proteases (33–35). Serpins harbor protease recognition sequences and upon cleavage stay covalently bound to the target proteases via acyl-enzyme intermediates. This covalent inhibition is achieved through dramatic post-cleavage strand insertion in serpins, which result in deformation and denaturation of the protease active sites and therefore the trapping of the acyl-enzyme intermediates from being hydrolyzed by the proteases (35).

While the exact structural basis of covalent protease inhibition is different in the two cases, there are several remarkable mechanistic similarities. First, both serpins and p35 undergo dramatic conformational changes, or refolding, upon cleavage. Second, they both exhibit wide spectrum protease inhibition, because the most important requirement for inhibition appears to be the existence of a protease recognition site. Third, the efficiency of protease inhibition both appears to be driven by the rate of post-cleavage conformational changes. In keeping with this observation, leakage in inhibition has been observed for both serpins and p35 (9, 33). Therefore, in either case, the inhibitory characteristic of the inhibitor is determined by the kinetic property of the system.

Acknowledgment—We thank Dr. Carl Nathan for the use of the SpectraMax Gemini plate reader.

REFERENCES

1. Thompson, C. B. (1995) *Science* **267,** 1456–1461
2. Johnstone, R. W., Ruefli, A. A., and Lowe, S. W. (2002) *Cell* **108,** 153–164
3. Nicholson, D. W. (1999) *Cell Death Differ.* **6,** 1028–1042
4. Stennicke, H. R., Renatus, M., Meldal, M., and Salvesen, G. S. (2000) *Biochem. J.* ***350,*** 563–568
5. Ekert, P. G., Silke, J., and Vaux, D. L. (1999) *Cell Death Differ.* **6,** 1081–1086
6. Stennicke, H. R., Ryan, C. A., and Salvesen, G. S. (2002) *Trends Biochem. Sci.* **27,** 94–101
7. Bump, N. J., Hackett, M., Hugunin, M., Seshagiri, S., Brady, K., Chen, P., Ferenz, C., Franklin, S., Ghayur, T., Li, P., Mankovich, J., Shi, L. F., Greenburg, A. H., Miller, L. K., and Wong, W. W. (1995) *Science* **269,** 1885–1888
8. Xue, D., and Horvitz, H. R. (1995) *Nature* **377,** 248–251
9. Zhou, Q., Krebs, J. F., Snipas, S. J., Price, A., Alnemri, E. S., Tomaselli, K. J., and Salvesen, G. S. (1998) *Biochemistry* **37,** 10757–10765
10. Araki, T., Shibata, M., Takano, R., Hisahara, S., Imamura, S., Fukuuchi, Y., Saruta, T., Okano, H., and Miura, M. (2000) *Cell Death Differ.* **7,** 485–492
11. Beidler, D. R., Tewari, M., Friesen, P. D., Poirier, G., and Dixit, V. M. (1995) *J. Biol. Chem.* **270,** 16526–16528
12. Clem, R. J., Fechheimer, M., and Miller, L. K. (1991) *Science* **254,** 1388–1390
13. Datta, R., Kojima, H., Banach, D., Bump, N. J., Talanian, R. V., Alnemri, E. S., Weichselbaum, R. R., Wong, W. W., and Kufe, D. W. (1997) *J. Biol. Chem.* **272,** 1965–1969
14. Hay, B. A., Wolff, T., and Rubin, G. M. (1994) *Development* (*Camb.*) **120,** 2121–2129
15. Hisahara, S., Araki, T., Sugiyama, F., Yagami, K., Suzuki, M., Abe, K., Yamamura, K., Miyazaki, J., Momoi, T., Saruta, T., Bernard, C. C., Okano, H., and Miura, M. (2000) *EMBO J.* **19,** 341–348
16. Martinou, I., Fernandez, P. A., Missotten, M., White, E., Allet, B., Sadoul, R., and Martinou, J. C. (1995) *J. Cell Biol.* **128,** 201–208
17. Morishima, N., Okano, K., Shibata, T., and Maeda, S. (1998) *FEBS Lett.* **427,** 144–148
18. Rabizadeh, S., LaCount, D. J., Friesen, P. D., and Bredesen, D. E. (1993) *J. Neurochem.* **61,** 2318–2321

19. Robertson, N. M., Zangrilli, J., Fernandes-Alnemri, T., Friesen, P. D., Litwack, G., and Alnemri, E. S. (1997) *Cancer Res.* **57,** 43–47
20. Sugimoto, A., Friesen, P. D., and Rothman, J. H. (1994) *EMBO J.* **13,** 2023–2028
21. Fisher, A. J., Cruz, W., Zoog, S. J., Schneider, C. L., and Friesen, P. D. (1999) *EMBO J.* **18,** 2031–2039
22. Xu, G., Cirilli, M., Huang, Y., Rich, R. L., Myszka, D. G., and Wu, H. (2001) *Nature* **410,** 494–497
23. Myszka, D. G. (1999) *J. Mol. Recognit.* **12,** 279–284
24. Myszka, D. G., and Morton, T. A. (1998) *Trends Biochem. Sci.* **23,** 149–150
25. Park, Y. C., Ye, H., Hsia, C., Segal, D., Rich, R. L., Liou, H.-L., Myszka, D. G., and Wu, H. (2000) *Cell* **101,** 777–787
26. Cunningham, B. C., and Wells, J. A. (1993) *J. Mol. Biol.* **234,** 554–563
27. Eddins, M. J., Lemongello, D., Friesen, P. D., and Fisher, A. J. (2002) *Acta Crystallogr. Sect. D Biol. Crystallogr.* **58,** 299–302
28. Snipas, S. J., Stennicke, H. R., Riedl, S., Potempa, J., Travis, J., Barrett, A. J., and Salvesen, G. S. (2001) *Biochem. J.* **357,** 575–580
29. Bertin, J., Mendrysa, S. M., LaCount, D. J., Gaur, S., Krebs, J. F., Armstrong, R. C., Tomaselli, K. J., and Friesen, P. D. (1996) *J. Virol.* **70,** 6251–6259
30. Thornberry, N. A., Rano, T. A., Peterson, E. P., Rasper, D. M., Timkey, T., Garcia-Calvo, M., Houtzager, V. M., Nordstrom, P. A., Roy, S., Vaillancourt, J. P., Chapman, K. T., and Nicholson, D. W. (1997) *J. Biol. Chem.* **272,** 17907–17911
31. Zoog, S. J., Bertin, J., and Friesen, P. D. (1999) *J. Biol. Chem.* **274,** 25995–26002
32. dela Cruz, W. P., Friesen, P. D., and Fisher, A. J. (2001) *J. Biol. Chem.* **276,** 32933–32939
33. Wright, H. T., and Scarsdale, J. N. (1995) *Proteins* **22,** 210–225
34. Engh, R. A., Huber, R., Bode, W., and Schulze, A. J. (1995) *Trends Biotechnol.* **13,** 503–510
35. Huntington, J. A., Read, R. J., and Carrell, R. W. (2000) *Nature* **407,** 923–926